How to cite: *Angew. Chem. Int. Ed.* **2020**, *59*, 21230–21235
International Edition: doi.org/10.1002/anie.202010634
German Edition: doi.org/10.1002/ange.202010634

Surface Chemistry | Hot Paper

# Cooperation of N-Heterocyclic Carbenes on a Gold Surface

*Saeed Amirjalayer,* Anne Bakker, Matthias Freitag, Frank Glorius, and Harald Fuchs*

***Abstract:*** *Atomically precise tailoring of interface structures is crucial for developing functional materials. We demonstrate an N-heterocyclic carbene (NHC) based molecular tool, which modifies the structure of a gold surface with atomic accuracy by the formation of gold nanorods. After adsorption on the gold surface, individual surface atoms are pulled out by the NHCs, generating single-atom surface defects and mobile NHC-Au species. Atomistic calculations reveal that these molecular "ballbots" can act as assembling tools to dislocate individual surface atoms. The predicted functionality of these carbene-based complexes is confirmed by scanning tunneling microscopy measurements. Cooperative operation of these NHC-Au species induces a step-wise formation of gold nanorods. Consequently, the surface is re-structured by a zipper-type mechanism. Our work presents a foundation to utilize molecular-based nanotools to design surface structures.*

## Introduction

Nanoscale tools, enabling precise tailoring of the surface structure at the atomic level, provide direct access to steer interfacial processes. For example, the chemical, physical and even pharmaceutical properties[1] of gold distinctively depend on its surface termination. Since the activity and functionality are dominated by molecular phenomena at the interface, modifications of the surface structure—ultimately with atomic accuracy—play a key role for the development of functional materials for applications such as catalysis and sensing.[2] Molecular sized tools, performing specific tasks at the surface, could alter the interface locally with atomic precision. This enables the construction of suitable local environments at the surface with designated chemical and physical properties and thus tailor the resulting functionality in a massively parallel way in a bottom-up approach.

Over the past years a number of molecules have been developed which can influence for example, molecular packing[3] or diffusion[4] due to their controlled motion. In order to tailor the atomic surface structure, one of the main challenges is to engineer a nanoscale tool which combines strong surface interaction with high surface mobility. N-Heterocyclic carbenes (NHCs) have extensively been studied as ligands for metal complexes and exhibit strong impact on the chemical and physical properties of the metal center.[5] More recently, their interactions with metal surfaces have been investigated.[6] Previously, we reported that NHCs adsorbed on a Au(111) surface generate ballbot-type molecular species. In this case, the NHC is bound to a single gold adatom,[6d] which resulted in highly ordered and stable monolayers.[6b] Here, we use NHCs adsorbed on a reconstructed Au(110) $(2\times1)$ surface (Figure 1a) to induce a significantly different dynamics at the surface. In fact, at the facetted Au(110) $(2\times1)$ surface the carbene molecules not only pull out single gold atoms from the surface to form ball-bot type species, but in addition reconfigure the local environment of the created point defect by subsequently moving a specific second atom. The coordinated interplay of these carbene-Au species along the [110] direction results in step-wise restructuring of the surface by creating Au-nanorods.

We combined atomistic simulations with scanning tunneling microscopy (STM) measurements to decipher the two-step operating mode of such a carbene-based tool, which includes: (a) atomically defined etching and (b) a well-defined one-dimensional rearrangement of surface atoms. Using only mild thermal activation, these two steps can be well controlled. More importantly, the whole mechanism proceeds self-propelling and induces a cascade-type restructuring, which results in a successive long-range one-dimensional modification of the metal surface. By identifying intermediate states of the push-pull mechanism our theoretical and experimental investigations show that a step-wise transition from the Au(110)$(2\times1)$ surface to a "Au(110) $(3\times1)$-added row (AR)" surface is obtained. It should be noted that such a strategy is fundamentally different from previously reported reconstruction processes of metal surfaces, where thermal treatment, electrochemical treatment, or functionalization by self-assembled monolayers were used.[7] Although in the majority of these cases the detailed reconstruction mechanism is not known, in general a transition of the surface structure is associated with a change of the overall surface energy. Such a sudden transition hinders a precise and well-controlled local modification of the surface structure. In

[*] S. Amirjalayer, A. Bakker, H. Fuchs
Physikalisches Institut, Westfälische Wilhelms-Universität
Wilhelm-Klemm-Straße 10, 48149 Münster (Germany)
and
Center for Nanotechnology
Heisenbergstraße 11, 48149 Münster (Germany)
E-mail: s.amirjalayer@wwu.de
S. Amirjalayer
Center for Multiscale Theory and Computation, Westfälische Wilhelms-Universität
Corrensstraße 40, 48149 Münster (Germany)
M. Freitag, F. Glorius
Organisch-Chemisches Institut, Westfälische Wilhelms-Universität
Corrensstraße 40, 48149 Münster (Germany)
Supporting information and the ORCID identification number(s) for the author(s) of this article can be found under: https://doi.org/10.1002/anie.202010634.

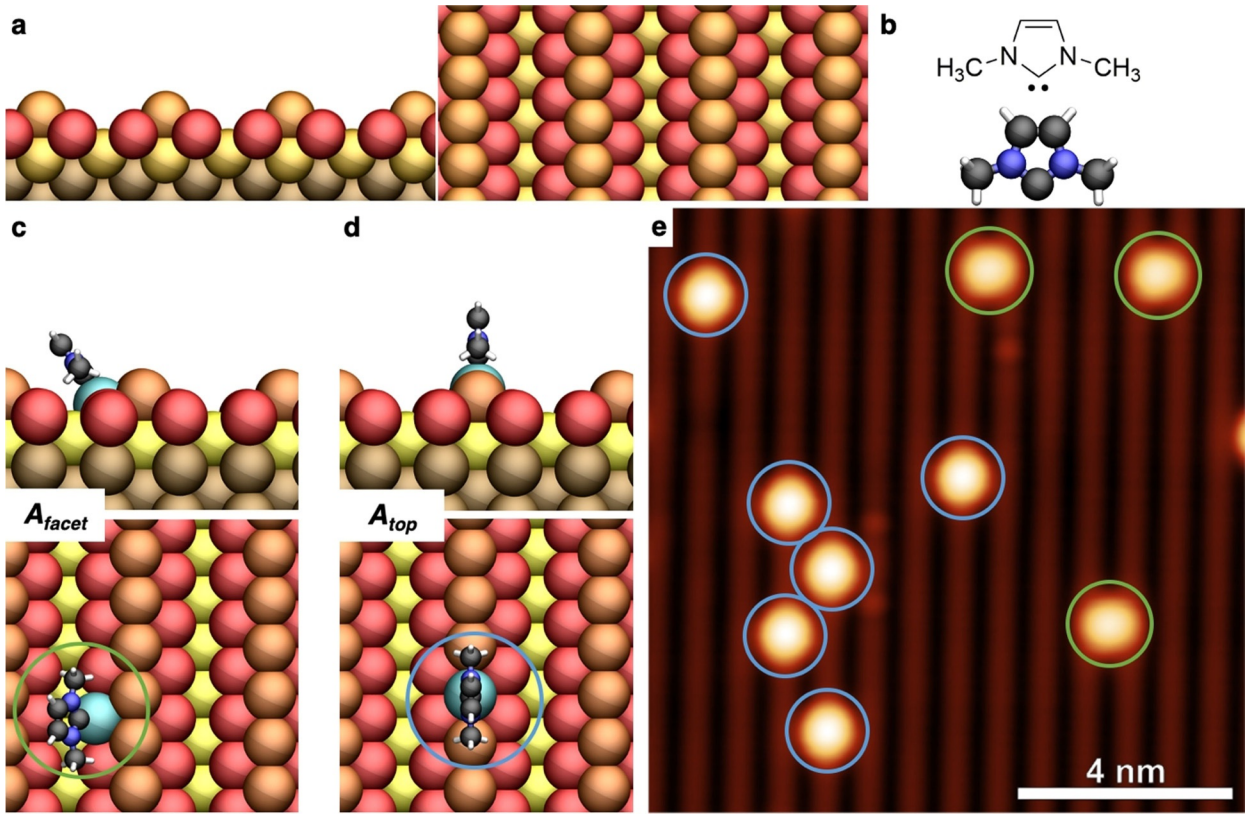


***Figure 1.*** a) Ball-and-stick model of the Au(110) (2×1) surface (top and side view; top-row: orange, facet-row: red, bottom-row: yellow, bulk-Au: ochre; for clarity cyano: gold atom bonded to the IMe in the adsorbed state (***A***)) and b) Lewis-structure together with the ball-and-stick model of the IMe molecule. c)–e) Initial adsorption of IMe at the gold surface: Ball-and-stick models (top and side view, carbon: black, nitrogen: blue, hydrogen: white) of $\boldsymbol{A}_{facet}$ (c) and $\boldsymbol{A}_{top}$ (d) together with an STM image of the Au(110) (2×1) surface covered with a low concentration of IMe (−1 V, 50 pA): top-row blue, bridge-row green (e).

contrast to this, our NHC-based molecular tool, which builds up gold nanorods and therefore reshapes the interfacial structure specifically, provides direct access to design complex surfaces for specific applications such as catalysis.

## Results and Discussion

In our investigation we focused on IMe (Figure 1b), which has been investigated on non-reconstructed Au surfaces.[6d,g,i,j] In line with the known strong interaction of NHCs with gold atoms, our atomistic simulations show a strong binding of IMe to the Au(110) (2×1) surface. However, at this reconstructed surface the atoms exhibit three different coordination environments (Figure 1a), which results in an energetic hierarchy of the adsorption sites of IMe (***A***). The adsorption on a gold atom in the *facet-row* ($\boldsymbol{A}_{facet}$, Figure 1c) and at the *top-row* ($\boldsymbol{A}_{top}$, Figure 1d) positions are energetically preferred, as compared to the bottom row position. In order to validate the predicted adsorption positions, STM measurements of a Au(110) (2×1) substrate (see SI, Figure S2) covered with a low concentration of IMe are performed (Figure 1e) following our previously reported gas-phase deposition approach in ultra-high vacuum.[6d] The obtained high-resolution STM images confirm the theoretical results. Despite the strong binding, the adsorbed IMe has some degree of flexibility for example, bending and rotation at the top-row position resulting in different configurations (see SI, Figure S3), which will lead to entropic contributions in addition to the calculated energetics. A statistical analysis of the STM images reveals that 68% of the IMe molecules adsorbs at the *top-row* position and 32% at the *facet-row* position, which can be assigned to the calculated $\boldsymbol{A}_{top}$ and $\boldsymbol{A}_{facet}$ position, respectively (Figure 1c,d and see SI, S3).

Due to the strong carbene-gold binding no mobility of solely the IMe molecule was observed during the STM measurements performed at 77 K (Figure 1b and see SI, Figure S4). Therefore, we explored in a next step the dynamics of IMe on Au(110) by evaluating whether it can form an IMe-Au species by pulling out a gold atom as was reported for Au(111).[6d] We calculated the energy profile for the pulling out process, considering the energetically preferred and experimentally observed adsorption sites. Our atomistic simulations reveal that IMe can pull out a gold atom to create a single-atom surface defect and an IMe-Au molecular ballbot (***B***) located at the facets of the Au(110) (2×1) surface ($\boldsymbol{B}_{facet}$, Figure 2a). The transition barrier for this nano-etching process ($\Delta E^{+}(\boldsymbol{A}_{facet} \rightarrow \boldsymbol{B}_{facet}) = 167.2$ meV (see SI, Figure S5) and $\Delta E^{+}(\boldsymbol{A}_{topB} \rightarrow \boldsymbol{B}_{facet} = 174.6$ meV) is lower compared to previously reported values for on-surface chemical reaction occurring at room temperature, which indicate that such processes are energetically feasible.[8]

  

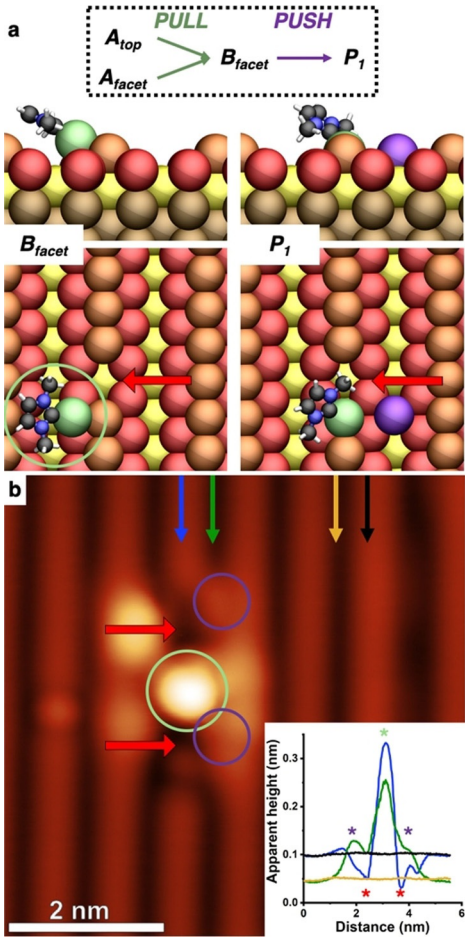


***Figure 2.*** a) Reaction scheme for the formation of the molecular ballbot ($B_{facet}$) and the subsequent pushing out of a gold atom from the top-row of the trench by the IMe-Au species ($P_1$) and the corresponding ball-and stick model (side and top view; The same color coding as in Figure 1 is used; for clarity green: gold atom of the ballbot species, violet: gold atom moved into the trench, red arrow: created surface defect). b) STM image after 31 h at room temperature (−1.2 V, 50 pA) together with height profiles (inset: Yellow/black: intact trench/top row; green/blue: defect trench/top row; −1.2 V, 50 pA) showing experimental evidence for the formation of atomically precise defects and single-atom dislocations. For comparison the same color coding as in the theoretical results was used to highlight the areas in the STM image and height profile. Both lines profiles are dominated by the central protrusion of an IMe-Au species. However, at the sides, the blue profile (top row) is reduced to trench level (yellow) and the green profile (trench) is increased to top row-level (black) indicating that atoms moved from the top row in the trench.

Importantly and in contrast to the Au(111) surface, no indication for simultaneous refilling of the surface defect by the underlying gold atoms was found here.

As we will show in the following, unlike the initially adsorbed IMe, the generated molecular ballbot ($B_{facet}$) shows distinct mobility at the surface. The IMe-Au species can diffuse parallel to the Au(110) (2 × 1) reconstruction along the facets ($\Delta E^{\ddagger} = 113.8$ meV, see SI, Figure S6) or along the trenches ($\Delta E^{\ddagger} = 407.4$ meV, see SI, Figure S6). Thus, enabling to transport the carbene-bound Au atom away from the created surface defect. It should be noted that the local density of surface atoms is decreased due to the dynamics of these IMe-Au species. Interestingly, when investigating the mobility perpendicular to the trenches we discovered a thermally accessible pushing motion towards individual gold atoms from the *top-row* position by the molecular ballbot ($\Delta E^{\ddagger} = 624.0$ meV, see SI, Figure S6). The dislocated Au atom is pushed into the trenches of the Au(2 × 1) surface and at the same time the IMe-Au occupies the *top-row* position (Figure 2a). For a bare metal substrate, a similar process at the step-edges has been described as an exchange mechanism to overcome the Ehrlich-Schwoebel barrier.[9] Evidently, the carbene-Au species is able to move single gold atoms via a similar mechanism.

To validate the thermally activated operation mode of the carbene-based tool, the prepared IMe-Au(110) system (Figure 1e) was inspected by STM after keeping the sample 31 h at room temperature (RT). In agreement with the calculations, the obtained STM images clearly show that individual surface atoms are missing from the *top-row* of the (2 × 1) reconstruction (Figure 2b and see SI, S7). In addition, height profiles measured along both intact and defect top rows and trenches confirm the dislocation of metal atoms into the (2 × 1) trench (Figure 2b insert). It should be emphasized that these types of surface defects and local rearrangements were never observed on the clean Au(110) surface. In all cases IMe-Au species can be identified around each defect demonstrating their involvement in the process. Moreover, the STM measurements (Figure 2b and see Si, S7) indicate that multiple IMe-Au-based molecular ballbots can work together to modify the surface structure beyond point defects.

Therefore, we subsequently investigated the interplay of multiple IMe-Au species together. In particular we studied how two ball-bots can coordinatively operate in order to transfer the atomically precise dislocation of individual gold atoms into long-range restructuring of the surface. Such a coordinated operation of the carbene molecules, which will be discussed in detail below, goes beyond the previously reported defect formations by adsorbed molecules at surfaces, where no long range restructuring of the surface was reported.[10] Using an extended model system including two IMe molecules revealed a smooth energy profile for an oscillatory movement of the IMe-Au species perpendicular to the trenches (Figure 3a and see SI, S8). This results in the formation of a gold nanorod by repeatedly dislocating surface atoms. As the molecular ballbots move both along the trenches and into and out of the top-row of the Au(110) (2 × 1) surface, the operation mode can be subdivided into alternating pulling and pushing steps (Figure 3a). Based on this, the two IMe-Au species step-wise restructure the gold surface creating a Au(110) (3 × 1) added row (AR) domain by merging two (2 × 1) top-rows together (Figure 3a). In this context it should be emphasized once again that due to the dynamics of the IMe-Au species along the trenches of the surface the local density of surface atoms is decreased.

Corresponding STM experiments provide direct evidence for this carbene-induced process (Figure 3b) and confirm the widening of the surface trenches (Figure 3b insert and see SI, S7). Going beyond this initial stage, the STM experiments further confirm the large-scale restructuring at the surface

  

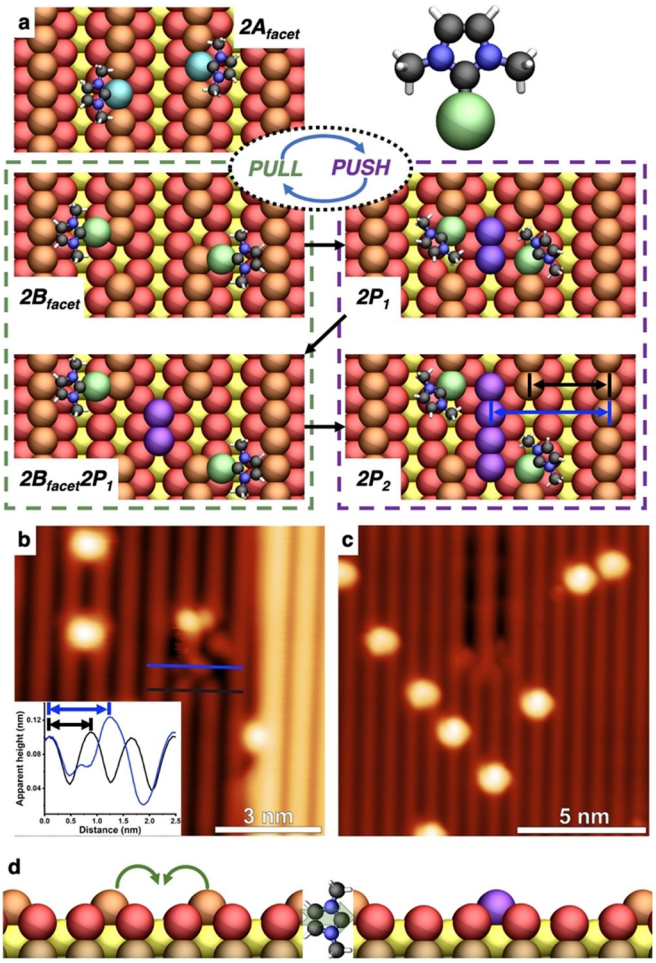


***Figure 3.*** a) Ball-and-stick representation of the underlying restructuring process (top-view), which can be described by alternating pulling (green box) and pushing steps (violet box) performed by the IMe-Au species, as the active nanoscale tool (top right). (The same color coding as in the previous Figures 1 and 2 is used.) b) STM image after the initial steps of the restructuring process (−1.2 V, 50 pA), in which two neighboring top rows contain defects and gold atoms are present in the middle between the (2×1) rows. The transition from a (2×1) to a (3×1) AR trench is further supported by the height profiles (inset: −1.2 V, 50 pA), which are in agreement with the change of the surface structure predicted by the atomistic simulation (blue and black arrows). c) STM image showing the result of the long-range zipping process (−1.3 V, 50 pA), in which two newly formed (3×1) AR trenches result from shifting top-row atoms in the center of a (2×1) trench and d) Ball-and-stick representation of the overall process.

terraces (Figure 3c and see SI, S9–10), which is in agreement with the self-propelling zipping-type restructuring of the surface (Figure 3d).

After understanding the mechanism of the IMe-Au-based nanoscale tool, we performed extended STM experiments to explore the parameter space to control the restructuring process. At first the effect of IMe coverage on the restructuring was investigated by depositing a low (0.09 mol nm$^2$), middle (0.26 mol nm$^2$) and high (0.42 mol nm$^2$) coverage of IMe on Au(110) (all in the sub-monolayer regime). The corresponding STM images (Figure 4a–c) and statistical analysis of the primary adsorption position (Figure 4g, see SI) clearly point out and quantify the correlation between surface restructuring and the amount of adsorbed IMe molecules. With increasing coverage, the percentage of IMe molecules adsorbing at the *top-row* position, which is assigned as the starting point of the zipping process, decreases significantly from 70% to 10% (Figure 4g) while, due to the reconstructing of the surface, an increase of the population in the (3×1) trench position is observed. (Figure 4c).

In a next step, we investigated the influence of time on this process by measuring repeatedly samples kept at RT for a certain number of hours (Figure 4d–f, h). Initially, the majority of IMe adsorbed in the $A_{top}$ (ca. 59%) and $A_{bridge}$ (ca. 38%) state and only very few molecules are observed in the (3×1) trenches (Figure 4h). After 14 hours this distribution significantly changes and the number of molecules in the (3×1) trenches jumps to 50%. This trend, which is a consequence of the restructuring of the surface, further proceeds resulting in around 70% in the trenches of the (3×1) surface areas after 60 hours (Figure 4h). These experimental results further confirm the thermally induced generation of mobile carbene-Au species and their coordinative operation to reshape the surface. It should be mentioned that, at higher coverage and with increasing time the formation of additional Au-nanorod-like structures on top of the restructured surface is observed. This again emphasizes the activity of the carbene molecules and their ability to modify the surface structure.

Further analysis of the STM results revealed a reduction of the amount of carbene species at the surface to 18% of the initial coverage after 125 hours, probably due to the formation of IMe-Au-IMe complexes,[6h] which might have a lower binding energy compared to the IMe-Au species. However, the exact desorption process might involve a more complex pathway, which is not in the scope of the current study. Despite desorption of the molecules, the modified surface persists and includes extended Au-nanorod-like structures, which even continue over step-edges (Figure 4i). Consequently, atomically precise modified surface structures can be constructed already at RT by employing these IMe-Au species, which is crucial to design interfacial structures for functional materials.

## Conclusion

In summary, a molecular-based nanoscale tool was created by adsorbing NHC molecules on the Au (110) (2×1) surface. Our experimental and theoretical investigations reveal that these nanoscale tools repeatedly perform two well-defined tasks at the surface. This includes first the generation of atomically defined surface defects by removing individual surface atoms and secondly the dislocation of single gold atoms by a pushing mechanism. We could further show by atomistic calculations and STM measurements that, based on this operating mechanism, these carbene-Au species can cooperate to construct gold nanorods at the surface. Following this process, we exhibit a long-range restructuring of the surface structure by the functionality of these molecular ballbots. The atomically precise reshaping of the surface occurs via a zipper-type mechanism. Importantly, this process

  

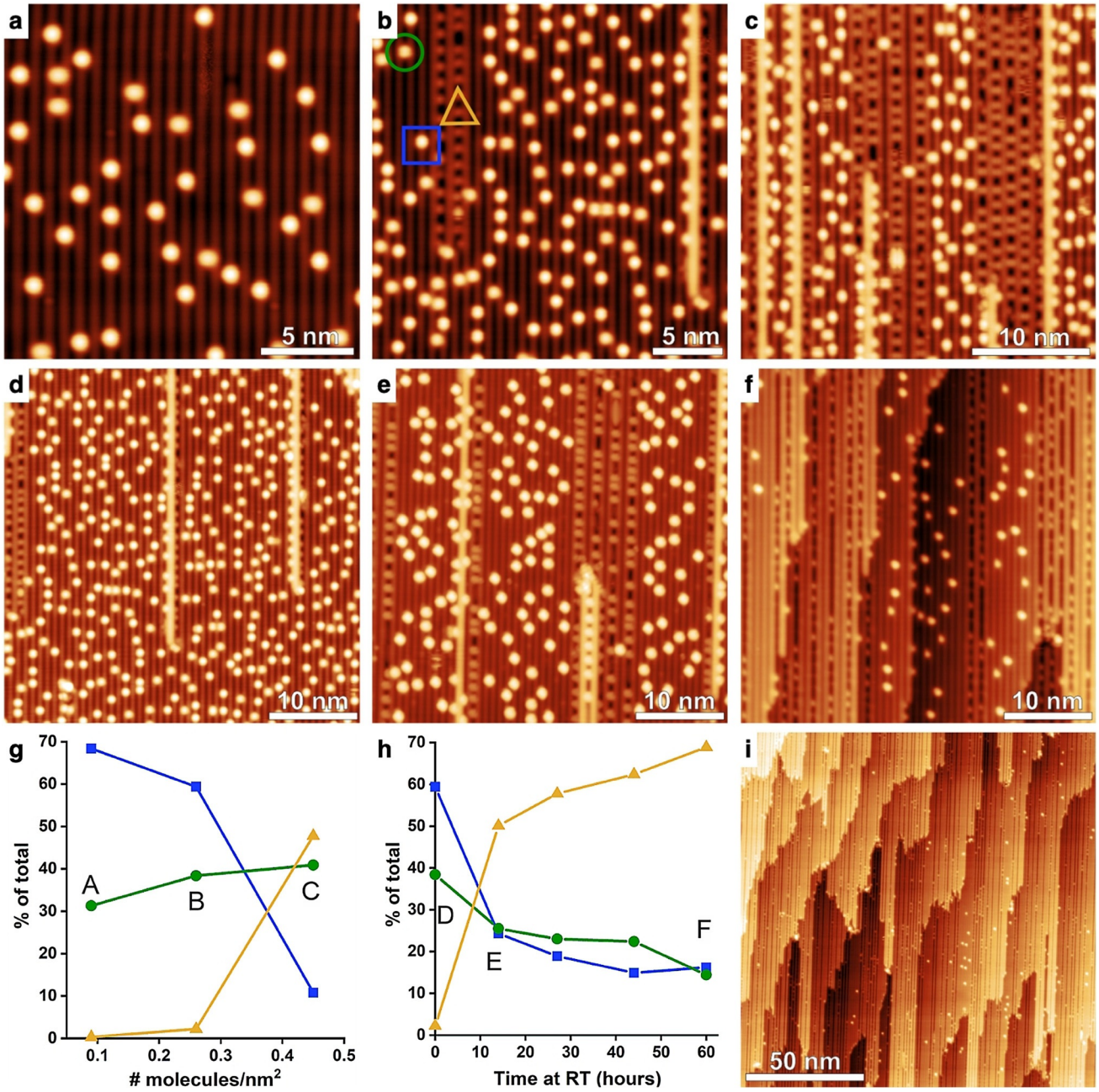


***Figure 4.*** a)–c) STM images at low (a, −1 V, 30 pA), middle (b, −1 V, 20 pA), and high concentrations (c, −1.2 V, 30 pA) of IMe on the Au(110) surface. d)–f) STM images of the middle coverage sample after 0 hours (d, −1 V, 20 pA), 14 hours (e, −2 V, 30 pA), and 60 hours (f, −2 V, 30 pA) at room temperature. g),h) A statistical analysis of three different adsorption positions ($A_{top}$ (blue), $A_{bridge}$ (green), and trench (3×1) (yellow), see Figure S11) as a measure of the restructuring process. The distribution over the three adsorption positions is plotted as a function of coverage (g) and as a function of time at room temperature for the middle coverage sample (h). The corresponding STM images are indicated in the plot. i) STM image of the middle coverage sample after 125 hours at room temperature showing that the (3×1) trenches persist after IMe desorbs (−1.7 V, 30 pA).

already takes place at room temperature and only in the presence of the NHC-Au complexes, which operate already at very low coverage and desorb after the restructuring of the surface. Both factors are fundamental to design interfacial structures for functional materials.

## Acknowledgements

We thank Dr. Harry Mönig for helpful discussions. This work was generously supported by the German research foundation through projects AM 460/2-1, FU 299/19 and the collaborative research centers SFB 858 (project B03) and TRR61 (B3, B7). Open access funding enabled and organized by Projekt DEAL.

  

## Conflict of interest

The authors declare no conflict of interest.

**Keywords:** atomistic simulation · nanoscale tools · N-heterocyclic carbenes · scanning tunneling microscopy · surface restructuring

[1] a) R. Wilson, *Chem. Soc. Rev.* **2008**, *37*, 2028 – 2045; b) J. Gong, *Chem. Rev.* **2012**, *112*, 2987 – 3054; c) Q. Zhang, L. Han, H. Jing, D. A. Blom, Y. Lin, H. L. Xin, H. Wang, *ACS Nano* **2016**, *10*, 2960 – 2974.

[2] a) I. Lee, F. Delbecq, R. Morales, M. A. Albiter, F. Zaera, *Nat. Mater.* **2009**, *8*, 132 – 138; b) J. W. Hong, S. U. Lee, Y. W. Lee, S. W. Han, *J. Am. Chem. Soc.* **2012**, *134*, 4565 – 4568; c) L. Liu, A. Corma, *Chem. Rev.* **2018**, *118*, 4981 – 5079; d) W. Huang, W. X. Li, *Phys. Chem. Chem. Phys.* **2019**, *21*, 523 – 536.

[3] R. Eelkema, M. M. Pollard, J. Vicario, N. Katsonis, B. S. Ramon, C. W. Bastiaansen, D. J. Broer, B. L. Feringa, *Nature* **2006**, *440*, 163.

[4] N. Liu, Z. Chen, D. R. Dunphy, Y. B. Jiang, R. A. Assink, C. J. Brinker, *Angew. Chem. Int. Ed.* **2003**, *42*, 1731 – 1734; *Angew. Chem.* **2003**, *115*, 1773 – 1776.

[5] a) M. N. Hopkinson, C. Richter, M. Schedler, F. Glorius, *Nature* **2014**, *510*, 485 – 496; b) A. V. Zhukhovitskiy, M. J. MacLeod, J. A. Johnson, *Chem. Rev.* **2015**, *115*, 11503 – 11532; c) C. A. Smith, M. R. Narouz, P. A. Lummis, I. Singh, A. Nazemi, C. H. Li, C. M. Crudden, *Chem. Rev.* **2019**, *119*, 4986 – 5056.

[6] a) A. V. Zhukhovitskiy, M. G. Mavros, T. Van Voorhis, J. A. Johnson, *J. Am. Chem. Soc.* **2013**, *135*, 7418 – 7421; b) C. M. Crudden, J. H. Horton, I. I. Ebralidze, O. V. Zenkina, A. B. McLean, B. Drevniok, Z. She, H. B. Kraatz, N. J. Mosey, T. Seki, E. C. Keske, J. D. Leake, A. Rousina-Webb, G. Wu, *Nat. Chem.* **2014**, *6*, 409 – 414; c) C. M. Crudden, J. H. Horton, M. R. Narouz, Z. Li, C. A. Smith, K. Munro, C. J. Baddeley, C. R. Larrea, B. Drevniok, B. Thanabalasingam, A. B. McLean, O. V. Zenkina, I. I. Ebralidze, Z. She, H. B. Kraatz, N. J. Mosey, L. N. Saunders, A. Yagi, *Nat. Commun.* **2016**, *7*, 12654; d) G. Wang, A. Ruhling, S. Amirjalayer, M. Knor, J. B. Ernst, C. Richter, H. J. Gao, A. Timmer, H. Y. Gao, N. L. Doltsinis, F. Glorius, H. Fuchs, *Nat. Chem.* **2017**, *9*, 152 – 156; e) C. Y. Wu, W. J. Wolf, Y. Levartovsky, H. A. Bechtel, M. C. Martin, F. D. Toste, E. Gross, *Nature* **2017**, *541*, 511 – 515; f) C. R. Larrea, C. J. Baddeley, M. R. Narouz, N. J. Mosey, J. H. Horton, C. M. Crudden, *ChemPhysChem* **2017**, *18*, 3536 – 3539; g) L. Jiang, B. Zhang, G. Medard, A. P. Seitsonen, F. Haag, F. Allegretti, J. Reichert, B. Kuster, J. V. Barth, A. C. Papageorgiou, *Chem. Sci.* **2017**, *8*, 8301 – 8308; h) A. Bakker, A. Timmer, E. Kolodzeiski, M. Freitag, H. Y. Gao, H. Monig, S. Amirjalayer, F. Glorius, H. Fuchs, *J. Am. Chem. Soc.* **2018**, *140*, 11889 – 11892; i) D. T. Nguyen, M. Freitag, M. Korsgen, S. Lamping, A. Ruhling, A. H. Schafer, M. H. Siekman, H. F. Arlinghaus, W. G. van der Wiel, F. Glorius, B. J. Ravoo, *Angew. Chem. Int. Ed.* **2018**, *57*, 11465 – 11469; *Angew. Chem.* **2018**, *130*, 11637 – 11641; j) A. Lv, M. Freitag, K. M. Chepiga, A. H. Schafer, F. Glorius, L. Chi, *Angew. Chem. Int. Ed.* **2018**, *57*, 4792 – 4796; *Angew. Chem.* **2018**, *130*, 4883 – 4887; k) G. Lovat, E. A. Doud, D. Lu, G. Kladnik, M. S. Inkpen, M. L. Steigerwald, D. Cvetko, M. S. Hybertsen, A. Morgante, X. Roy, L. Venkataraman, *Chem. Sci.* **2019**, *10*, 930 – 935; l) S. Dery, S. Kim, G. Tomaschun, I. Berg, D. Feferman, A. Cossaro, A. Verdini, L. Floreano, T. Kluner, F. D. Toste, E. Gross, *J. Phys. Chem. Lett.* **2019**, *10*, 5099 – 5104; m) Z. She, M. R. Narouz, C. A. Smith, A. MacLean, H. P. Loock, H. B. Kraatz, C. M. Crudden, *Chem. Commun.* **2020**, *56*, 1275 – 1278; n) J. Ren, M. Freitag, C. Schwermann, A. Bakker, S. Amirjalayer, A. Ruhling, H. Y. Gao, N. L. Doltsinis, F. Glorius, H. Fuchs, *Nano Lett.* **2020**, *20*, 5922 – 5928; o) A. Bakker, M. Freitag, E. Kolodzeiski, P. Bellotti, A. Timmer, J. Ren, B. Schulze Lammers, D. Moock, H. W. Roesky, H. Monig, S. Amirjalayer, H. Fuchs, F. Glorius, *Angew. Chem. Int. Ed.* **2020**, *59*, 13643 – 13646; *Angew. Chem.* **2020**, *132*, 13745 – 13749; p) D. T. Nguyen, M. Freitag, C. Gutheil, K. Sotthewes, B. J. Tyler, M. Bockmann, M. Das, F. Schluter, N. L. Doltsinis, H. F. Arlinghaus, B. J. Ravoo, F. Glorius, *Angew. Chem. Int. Ed.* **2020**, *59*, 13651 – 13656; *Angew. Chem.* **2020**, *132*, 13754 – 13759.

[7] a) B. M. Ocko, G. Helgesen, B. Schardt, J. Wang, A. Hamelin, *Phys. Rev. Lett.* **1992**, *69*, 3350 – 3353; b) X. P. Gao, M. J. Weaver, *Surf. Sci.* **1994**, *313*, L775 – L782; c) V. Mazine, Y. Borensztein, *Phys. Rev. Lett.* **2002**, *88*, 147403; d) A. Cossaro, D. Cvetko, G. Bavdek, L. Floreano, R. Gotter, A. Morgante, F. Evangelista, A. Ruocco, *J. Phys. Chem. B* **2004**, *108*, 14671 – 14676; e) D. Zhong, J. H. Franke, S. K. Podiyanachari, T. Blomker, H. Zhang, G. Kehr, G. Erker, H. Fuchs, L. Chi, *Science* **2011**, *334*, 213 – 216; f) R. Foulston, S. Gangopadhyay, C. Chiutu, P. Moriarty, R. G. Jones, *Phys. Chem. Chem. Phys.* **2012**, *14*, 6054 – 6066; g) E. V. Iski, A. D. Jewell, H. L. Tierney, G. Kyriakou, E. C. H. Sykes, *Surf. Sci.* **2012**, *606*, 536 – 541; h) K. Yoshida, A. Kuzume, P. Broekmann, I. V. Pobelov, T. Wandlowski, *Electrochim. Acta* **2014**, *139*, 281 – 288; i) H. Walen, D.-J. Liu, J. Oh, H. J. Yang, Y. Kim, P. A. Thiel, *J. Phys. Chem. C* **2015**, *119*, 21000 – 21010; j) K. Sun, A. Chen, M. Liu, H. Zhang, R. Duan, P. Ji, L. Li, Q. Li, C. Li, D. Zhong, K. Mullen, L. Chi, *J. Am. Chem. Soc.* **2018**, *140*, 4820 – 4825; k) X. Zhao, H. Yan, R. G. Zhao, W. S. Yang, *Langmuir* **2002**, *18*, 3910 – 3915; l) Y. Jugnet, F. J. Cadete Santos Aires, C. Deranlot, L. Piccolo, J. C. Bertolini, *Surf. Sci.* **2002**, *521*, L639 – L644; m) X. Gao, M. J. Weaver, *Phys. Rev. Lett.* **1994**, *73*, 846 – 849.

[8] a) M. Bieri, M. T. Nguyen, O. Groning, J. Cai, M. Treier, K. Ait-Mansour, P. Ruffieux, C. A. Pignedoli, D. Passerone, M. Kastler, K. Mullen, R. Fasel, *J. Am. Chem. Soc.* **2010**, *132*, 16669 – 16676; b) O. Diaz Arado, H. Monig, H. Wagner, J. H. Franke, G. Langewisch, P. A. Held, A. Studer, H. Fuchs, *ACS Nano* **2013**, *7*, 8509 – 8515; c) H. Y. Gao, P. A. Held, S. Amirjalayer, L. Liu, A. Timmer, B. Schirmer, O. Diaz Arado, H. Monig, C. Muck-Lichtenfeld, J. Neugebauer, A. Studer, H. Fuchs, *J. Am. Chem. Soc.* **2017**, *139*, 7012 – 7019; d) C. X. Wang, J. L. Chen, C. H. Shu, K. J. Shi, P. N. Liu, *Phys. Chem. Chem. Phys.* **2019**, *21*, 13222 – 13229.

[9] a) J. D. Wrigley, G. Ehrlich, *Phys. Rev. Lett.* **1980**, *44*, 661 – 663; b) T. T. Tsong, C. L. Chen, *Nature* **1992**, *355*, 328 – 331; c) G. Antczak, G. Ehrlich, *Surf. Sci. Rep.* **2007**, *62*, 39 – 61; d) M. Jäckle, K. Helmbrecht, M. Smits, D. Stottmeister, A. Groß, *Energy Environ. Sci.* **2018**, *11*, 3400 – 3407.

[10] A. Kühnle, T. R. Linderoth, B. Hammer, F. Besenbacher, *Nature* **2002**, *415*, 891 – 893.

Manuscript received: August 3, 2020
Accepted manuscript online: August 21, 2020
Version of record online: October 4, 2020

  